Heat-prone neighbourhood typologies of European cities with temperate climate

Yehan Wu [*,a,b], Bardia Mashhoodi [a], Agnès Patuano [a], Sanda Lenzholzer [a], Laura Narvaez Zertuche [b], Andy Acred [b]

[a] *Landscape Architecture and Spatial Planning Group, Department of Environmental Sciences, Wageningen University & Research, the Netherlands*
[b] *Foster + Partners, London, United Kingdom*

ABSTRACT

Outdoor microclimates vary among different urban neighbourhoods depending on their morphological variations. The Local Climate Zone (LCZ) framework is a well-developed typomorphological classification used to capture the variation that characterises neighbourhood microclimates. However, it does not include detailed morphological parameters within neighbourhoods that have synergistic effects on microclimates. It is thus essential to develop neighbourhood typologies with detailed spatial descriptions. This study first identifies the LCZ in Amsterdam, London and Paris with the highest Land Surface Temperature (hereinafter referred to as the most heat-prone areas). Subsequently, parameters which are not covered by the LCZs were analysed, including building block's floor area ratio and shape factor, street canyon's orientation and Height-to-Width ratio, street total length, green space area, and tree cover ratio. The results show that LCZ 2-compact mid-rise areas are the most heat-prone. Employing K-means cluster analysis, four neighbourhood typologies are distinguished within the LCZ 2: mainly wide streets with N-S and E-W orientations, mainly narrow streets with N-S and E-W orientations, mainly narrow streets with NE-SW and NW-SE orientations, mainly wide streets with four orientations divided by 45°. These generalised neighbourhood typologies can be used as the basis for design interventions aiming at climate adaptation in heat-prone urban areas.

1. Introduction

European cities with temperate climates have been suffering more and more from heat stress. The 2003 summer heatwave caused an estimated 70,000 excess deaths across Europe (Robine et al., 2008). In the summer of 2019, exceptional heatwaves also occurred in Western Europe. According to the Centre for Research on the Epidemiology of Disasters, the European summer heatwave was regarded as the deadliest extreme event in 2019 with a total of approximately 2500 deaths in France, the Netherlands, the UK, and Belgium (measured by excess mortality) (Froment and Below, 2020). In mid-July of 2022, the UK hit the temperature above 40 °C, which is the highest on record since measurements started (Witze, 2022). Due to climate change, the intensity of urban heat stress and the likelihood of extreme weather

conditions are expected to increase in the near future (Raymond et al., 2017). This situation worsened, particularly in Western Europe, which becomes a hotspot for heatwaves (Witze, 2022; Rousi et al., 2022). Therefore, climate adaptation measures to prepare for the coming extreme weather conditions are essential. Within this context, transferable microclimate knowledge is needed for urban planners and policy makers in their decision-making process (Brown, 2010; Lenzholzer, 2015).

Interventions for urban climate adaptation are thus highly demanded, especially at the neighbourhood level. Indeed, the neighbourhood scale is where small and fast interventions can be implemented to achieve cooling effects (Roe & McCay, 2021). The neighbourhood scale is the level where local government plans are developed and implemented for microclimate improvement, yet research at this scale received

Table 1
Neighbourhood morphological parameters affecting microclimates.

Parameter type	Name of Parameter	Abbreviation	Definition	Reference	Included in LCZ
Block	Building coverage ratio	BCR	The ratio of the building area divided by the site area (footprint).	(Martins et al., 2019; Oke et al., 2017; Xu et al., 2017)	Yes
	Mean building height	MBH	The ratio of total heights of buildings of a given area to the number of the building in this area.	(Oke et al., 2017; Sangiorgio et al., 2020; Xu et al., 2017)	Yes
	Floor area ratio	FAR	The ratio of all buildings' total floor area (gross floor area) to the size of the piece of the land which the buildings were built.	(Pan, 2019; Rode et al., 2014; Maiullari et al., 2021)	No
	Shape factor	SF	The ratio of the perimeter of the patch to the equivalent circular perimeter of the same area. The larger the ratio, the more developed the periphery of the block.	(Liu et al., 2019; Louf & Barthelemy, 2014)	No
Street	Sky view factor	SVF	The percentage of visible sky.	(Oke et al., 2017; Xu et al., 2017)	Yes
	Height-to-Width ratio	H/W	The ratio of the height of buildings to the width of the street canyon.	(Ali-Toudert & Mayer, 2006; Chatzidimitriou & Yannas, 2017)	No
	Canyon axis orientation	CAO	The orientation of the street canyon.	(Ali-Toudert & Mayer 2006)	No
	Street length	SL	The total length of street in a given area.	(Knight & Marshall, 2015)	No
Vegetation	Tree cover ratio	TCR	The ground tree coverage of the given site.	(Rahman et al., 2019; Ziter et al., 2019; Kim & Brown, 2022)	No
	Greenspace area	AGS	The size of greenspace in a given area.	(Amani-Beni et al., 2018; Cohen et al., 2012; Perini & Magliocco, 2014)	No

limited attention (Norton et al., 2015; Bartesaghi-Koc et al., 2018). Given the impact of morphological characteristics on urban neighbourhoods' microclimates (Aghamolaei et al., 2020), quantitative descriptions of neighbourhoods' morphological parameters can support design interventions aiming at urban microclimate adaptation.

The concept of typomorphology (also known as typologies of urban surface properties) was proposed to describe the diversity of urban form characteristics and describe urban form in an integrative way that can effectively inform urban planning and design practices (Eldesoky et al., 2022; Berghauser Pont et al., 2019). Creating spatial representations of neighbourhood typologies can be used as a basis to plan or formulate design interventions, as design interventions require easily applicable knowledge that works beyond a specific case to a more generalisable set of situations (Lenzholzer & Brown, 2016; Prominski, 2016; Hidalgo et al., 2018). At a neighbourhood level, Local Climate Zones (LCZ) have been widely used as a typomorphological classification (Eldesoky et al., 2022; Bartesaghi-Koc et al., 2018; Middel et al., 2014; Yang et al., 2021; Zheng et al., 2018). Originally developed by Stewart & Oke (2012), LCZs categorise landscape characteristics into 17 different types based on generalised knowledge of built forms and land cover types and quantifiable measures.

The Local Climate Zone (LCZ) classification was developed as a universal description of local scale landscape types, distinguishing parameters that directly influence 2-m air temperature in the canopy layer (Stewart & Oke, 2012). The main parameters included in the LCZ classification are the ratio of building plan area to total plan area, ratio of impervious plan area (paved, rock) to total plan area, and ratio of pervious plan area (bare soil, vegetation, water) to total plan area, mean height of roughness elements (geometric average of building heights and tree/plant heights), sky view factor, and anthropogenic heat flux (Stewart & Oke, 2012). Many studies have shown the significant relationship between Land Surface Temperature (LST) and LCZ types (Bechtel et al., 2019; Cai et al., 2018), providing evidence to support the use of this classification as an effective tool to identify heat-prone areas in the city. The World Urban Database and Access Portal Tools (WUDAPT) platform made the LCZ classification an open tool to apply to cities worldwide (Demuzere et al., 2019). As it grew in popularity, the LCZ framework allowed the tackling of urban climate issues using a common language.

However, from the perspective of formulating design guidelines at the neighbourhood scale, the LCZ classification still has limitations. Currently, LCZs are typically considered as homogenous configurations (Stewart & Oke, 2012; Bechtel & Daneke, 2012). There is a lack of studies which identified the typomorphologies within an LCZ, which could also be called sub-LCZs. Indeed, LCZs only capture the variation in microclimates that characterises neighbourhoods of $\geq 1 km^2$ in cities (Bechtel et al., 2019). However, LCZs do not include a variety of other essential morphological parameters which potentially affect urban climate at the neighbourhood level, such as the micro-scale characteristics of block, street, and vegetation patterns.

Urban neighbourhoods are complex combinations of different micro-scale parameters that can have a synergistic effect on the microclimate (Ramyar et al., 2019; Yin et al., 2019; Aghamolaei 2020). Some researchers have identified typical street typologies with different height-width ratios (Aboelata, 2020; Chatzidimitriou & Yannas, 2017; Klemm et al., 2015; Srivanit & Jareemit, 2020) or building typologies including pavilions, slabs, courtyards etc., (Ratti et al., 2003; Taleghani et al., 2015). However, only focusing on certain streets or buildings cannot provide a holistic basis for urban designers to plan their interventions at a neighbourhood scale (Erell, 2008). Multiple factors, rather than single elements, need to be considered in urban climate research since the thermal environment is influenced by complex interactions of multiple factors in the urban environment (Aleksandrowicz et al., 2017; Yao et al., 2020; Yin et al., 2019; Elbondira et al., 2021). Although some researchers explored urban design parameters such as floor are ratio (FAR) and tree cover ratio (TCR) as quantitative descriptions to propose neighbourhood typologies (Maiullari et al., 2021), knowledge about how other parameters, such as the street orientations and H/Ws can be reflected at the neighbourhood scale is still lacking. Yet these two parameters are among the most influential factors in urban climate (Sangiorgio et al., 2020). Taking micro-scale design elements into account, Yin et al. (2019) identified neighbourhood typologies with different combinations of canyon types and layouts. Their simulation results show that synergistic effects exist among micro-scale elements in the neighbourhoods, and the favourable thermal sensation conditions were found in the neighbourhood with long East-West oriented arcade streets. Yet as mentioned in the limitations of their studies, there are many other parameters that need to be considered at the same time, such as the canopy ratio of greenery, the type of vegetation and four street orientations' combinations.

It is therefore important to consider morphological parameters for design interventions that are not yet included in the LCZ typologies. More detailed morphological parameters should cover key aspects of urban and architectural design, which are well known by architects and
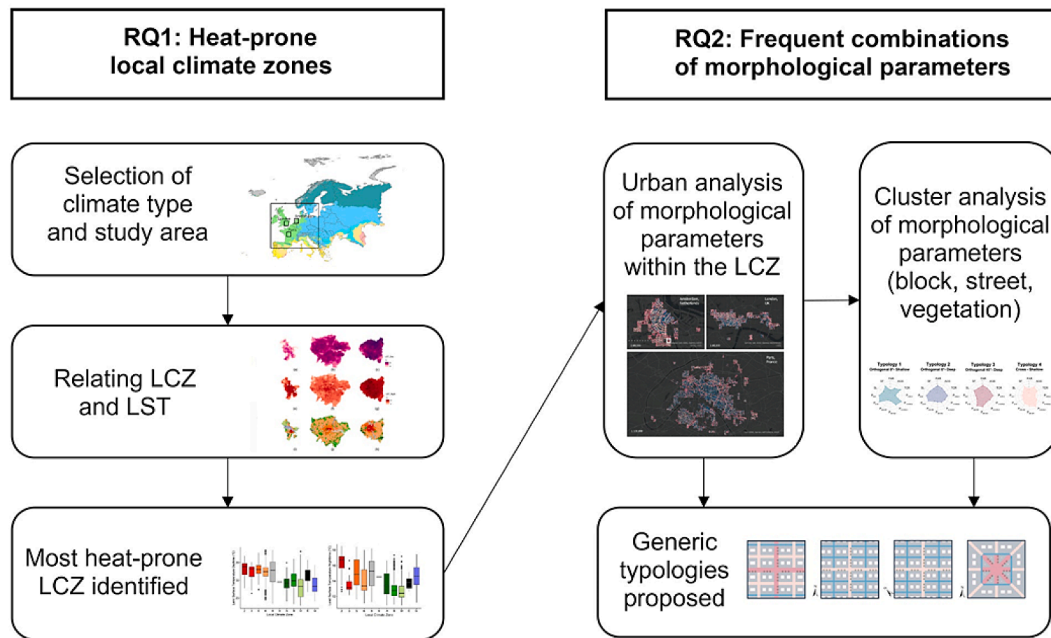
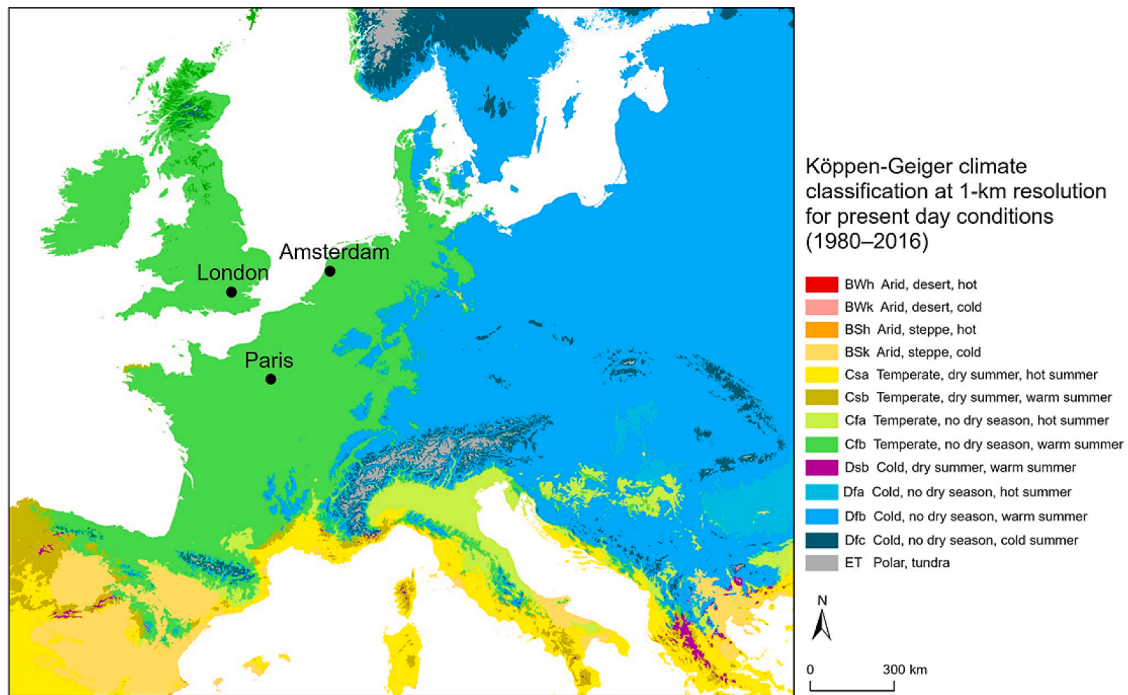**Fig. 1.** Methodological flowchart of the process of this research.

Fig. 2. Köppen-Geiger climate classification. This study focuses on Amsterdam, London, and Paris in the Cfb climate zone.

urban designers and can be efficiently utilised during both the pre-design stage and the post-occupancy evaluation period (Pan & Du, 2021). Based on existing studies, there are three types of parameters concerning block, street and vegetation that can influence microclimates (Table 1).

A city is constituted of various types of morphological patterns, and their components are difficult to understand in isolation (Demuzere et al., 2022). Under the current threat of severe heatwaves that are widespread across the world, the aim of this study is to propose a new analysis approach that identifies heat-prone neighbourhood typologies from real-world data. These typologies can act as a basis to plan or

formulate design interventions. To focus on the most problematic area, the widely adopted LCZ scheme is used for identifying the most heat-prone LCZ type. Considering that the LCZs that suffer urban heat require heat-mitigating measures, there is a necessity to analyse the micro-scale urban design parameters that influence microclimates. The objective of this study is to determine the combinations of micro-scale morphological parameters for the formulation of heat-prone neighbourhood typologies, assessing if there are significant morphological differences across the most heat-prone LCZ. To that end, the study puts forward two research questions: 1). What is the most heat-prone Local Climate Zone (LCZ) in European cities with temperate climate? 2). What

Table 2
Overview of neighbourhood morphological variables calculated in this study.

Parameter (unit)	Variable	Calculation per grid	Raw data
FAR (>0)	FAR	$BCR \times Floor$	**Building height** of Amsterdam (Peters et al., 2021), London (OS MasterMap Building Height Attribute, 2019), Paris (Atelier Parisien d'Urbanisme, 2020)
SF (>1)	SF	$0.5 \times Block\ Perimeter / \sqrt{\pi \times Block\ Size}$	
SL (metre)	SL	$Total\ street\ length$	
CAO	$P_{N\text{-}S}$	$Street\ length_{(N-S)}\ /\ SL$	
	$P_{E\text{-}W}$	$Street\ length_{(E-W)}\ /\ SL$	
	$P_{NW\text{-}SE}$	$Street\ length_{(NW-SE)}\ /\ SL$	
	$P_{NE\text{-}SW}$	$Street\ length_{(NE-SW)}\ /\ SL$	
H/W (>0)	$P_{0<H/W\leq1}$	$Street\ length_{(0<H/W\leq1)}\ /\ SL$	**Block, street, and green space polygon** (Urban Atlas 2018 — Copernicus Land Monitoring Service, 2020)
	$P_{1<H/W\leq2}$	$Street\ length_{(1<H/W\leq2)}\ /\ SL$	
	$P_{H/W>2}$	$Street\ length_{(H/W>2)}\ /\ SL$	**Tree canopy cover** (DiMiceli et al., 2015)
TCR (≥0)	TCR	$Tree\ canopy\ area\ /\ Grid\ size$	
AGS (m^2)	AGS	$Total\ green\ space\ area$	

are the most frequent neighbourhood typologies within the identified LCZ based on the characteristics of blocks, streets, and vegetation?

2. Methodology and data

The methodology of this study was designed to systematically capture empirical data of real urban settings with diverse morphological characteristics.

The methodology of this study consists of two main steps (Fig. 1): to answer the first research question of identifying heat-prone Local Climate Zone (LCZ), three European cities of Amsterdam, London, and Paris in the temperate climate zone (Cfb) were selected as study areas. Then the spatial data of Land Surface Temperature (LST) and LCZ within the three cities was overlapped and the LCZ with the highest level of LST was identified. To answer the second research question of identifying frequent neighbourhood typologies, each morphological parameter was first calculated and mapped within the identified heat-prone Local Climate Zone. K-means cluster analysis was then conducted to identify the frequent combinations of morphological parameters. Final generic typologies were developed based on the urban analysis values and cluster centres. All the spatial analysis was conducted and visualised in ArcGIS Pro 2.9. All the statistical analysis was conducted and visualised using IBM SPSS Statistics 26 and R Studio 1.4. In the following sections, the methods are described in detail.

2.1. Study area

This study focuses on the temperate climate zone in Europe, or Cfb (Temperate oceanic climate, warm summer and no dry season), according to the Köppen-Geiger classification (Fig. 2, Beck et al., 2018). Among the cities in Cfb, three cities were selected based on the following two criteria: (1) A city that includes as many different LCZ types as possible; (2) The availability of data on building geometry and heights, as well as block geometry. Based on these criteria, Amsterdam, London and Paris were selected as cases to identify representative neighbourhood typologies. Given the fact that urban heat island effects are most prominent at night when people mostly do activities within residential areas (Zhang et al., 2017; Deilami et al., 2018), this study only considers residential neighbourhoods as they need prioritised design interventions to improve microclimates.

2.2. Relating local climate zone and land surface temperature

To examine which Local Climate Zone (LCZ) type is most heat-prone across these three cities, Land Surface Temperatures (LST) was used as an indicator of heat stress (Bechtel et al., 2019). To spatially relate LCZ and LST data, LCZ was resampled to the same grid size of LST using the majority function in ArcGIS Pro 2.9. To compare the significant differences between the means of LST in different types of LCZ, a one-way ANOVA with post hoc Bonferroni test was conducted (Appendix A).

The data of the Local Climate Zone map was retrieved from the WUDAPT team's research on mapping European LCZs (Demuzere et al., 2019) which consists of open data with a resolution of 100 metres. The boundary of the three studied cities is based on the data from Urban Atlas Copernicus 2018. The Land Surface Temperature map that combines the data of three studied cities was produced based on the MODIS satellite data MOD11A2 and MYD11A2 (Wan et al., 2015) using Google Earth Engine. LST of four different overpassing at local times at each of the periods was retrieved: MODIS Terra day (10:30 a.m.), MODIS Terra night (10:30 p.m.), MODIS Aqua day (1:30 p.m.), and MODIS Aqua night (1:30 a.m.). The spatial resolution is 1 kilometre.

To identify the months these cities suffer most from heat stress in a year, we used the EnergyPlus Weather File (EPW) of climate data from the meteorological station of Amsterdam Schiphol, London Weather Centre St. James Park, and Paris Mont Souris (Climate.Onebuilding, 2021). It shows that June to August are the hottest months. The LST data from June 1st to August 31st 2020 was thus used to represent the hottest period of the year. The data of MODIS Terra day (10:30 a.m.) and MODIS Aqua day (1:30 p.m.) were averaged to represent daytime LST, and MODIS Terra night (10:30 p.m.) and MODIS Aqua night (1:30 a.m.) were averaged to represent nighttime LST.

Surface albedo, which indicates surface ability to reflect the incoming direct and diffused irradiance, is an important factor affecting the ground temperature (Mitraka et al., 2015). In the urban context, the relatively low albedo and subsequent more thermal energy storage in pavement tend to generate a more severe urban heat island effect, whereas the high albedo materials covering urban surfaces are able to counteract the temperature increase and thereby mitigate the urban heat island effects (Yuan et al., 2017; Chen et al., 2020). Considering that surface albedo is a significant factor in influencing the urban heat island effects (Sangiorgio et al., 2020), the surface albedo of the three cities was also analysed. This is to verify if the surface albedo is constant in the focused heat-prone LCZ, otherwise it needs to be included as a parameter for cluster analysis in the next step. MODIS albedo product MCD43A3 (Schaaf & Wang, 2015) was used to estimate the surface albedo in the three cites with a resolution of 500 metres with the time period from June 1st to August 31st 2020 aggregated. Shortwave broadband albedo was used to represent the surface albedo value (Liang, 2001; Schaaf & Wang, 2015). To compute the blue-sky albedo, white- and black-sky albedo was averaged to represent the results of surface albedo (Schwaab et al., 2021).

2.3. Cluster analysis for combinations of neighbourhood morphological parameters

In order to conduct cluster analysis, the study areas were split into homogeneous grids. The size of the grids is $300 \times 300m$ which, according to Aminipouri et al. (2019) and Yin et al. (2019), is suitable for neighbourhood-level climate studies. Using the vegetation canopy cover data (DiMiceli et al., 2015) as the basis, the heat-prone LCZ type of the three cities was divided into grids of $300 \times 300m$ area.

All the detailed morphological parameters analysed can be divided into three neighbourhood element types: block, street, and vegetation. The description, equation and data source of each parameter are presented in Table 2. All morphological parameters were analysed for the areas within the heat-prone LCZ in the three cities.

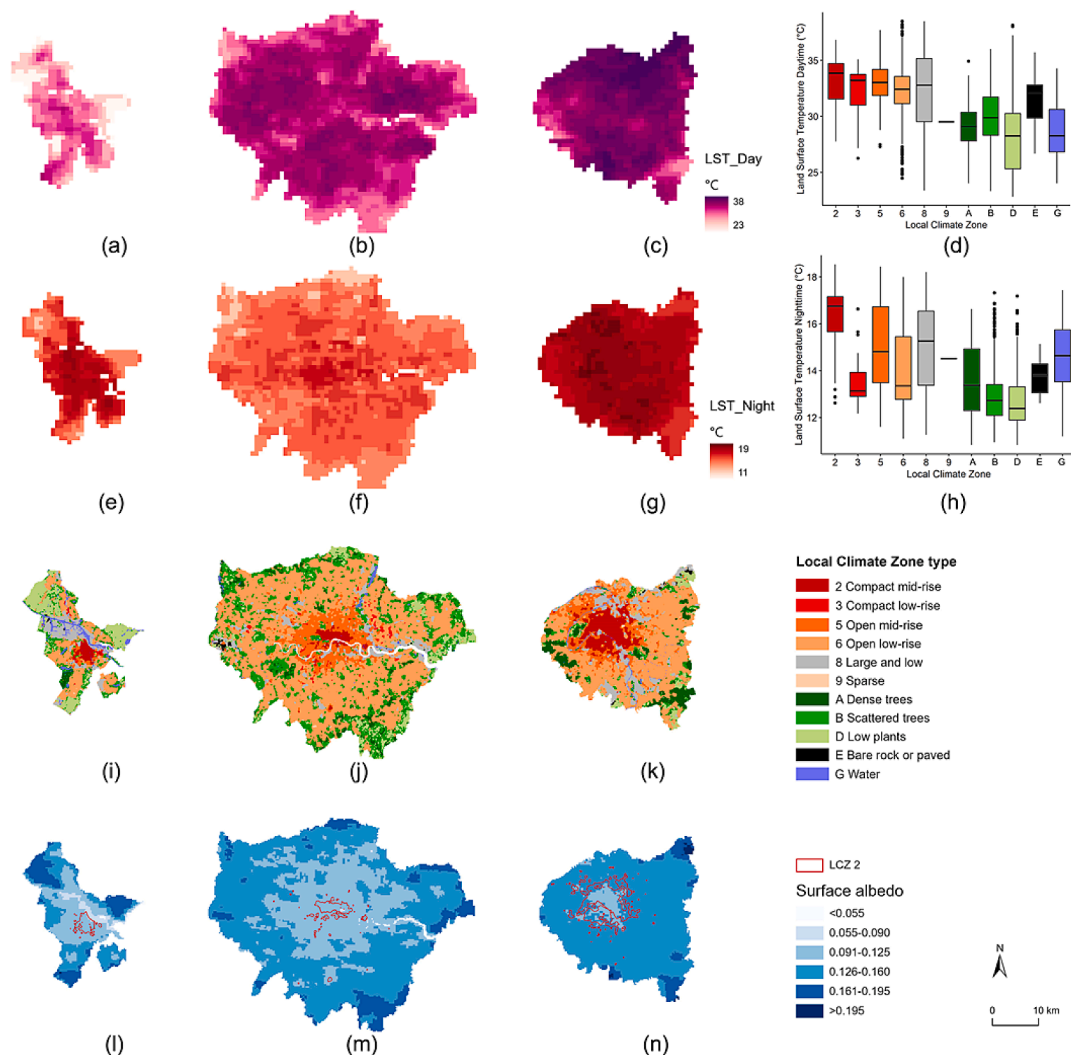Regarding block-related parameters, floor area ratio (FAR) and

Fig. 3. Daytime Land Surface Temperature (LST) in Amsterdam (a), London (b), and Paris (c). Nighttime LST in Amsterdam (e), London (f), and Paris (g). The boxplot of LST for daytime (d) and nighttime (h) both show that LCZ 2-compact mid-rise has the highest LST. Local Climate Zone (LCZ) types in Amsterdam (i), London (j), and Paris (k). LCZ 2 areas of the three cities are all situated in the city core, while the total area of LCZ 2 in Paris is much larger than in Amsterdam and London. Surface albedo in Amsterdam (l), London (m), and Paris (n).

shape factor (SF) were chosen. FAR is a building density indicator, influencing the magnitude of overheating and solar irradiance (Maiullari et al., 2021). Each block's FAR was calculated by multiplying the block's average floor and the block's building coverage ratio (BCR). BCR was calculated as the ratio of the building footprint inside one block and the area of the block. Each floor was 3 metres in mean building height (MBH) of the block. MBH was calculated as the mean height value of all the building heights. At the grid level, the FAR was calculated as the average FAR of the blocks inside the grid. SF reflects the length-to-width ratio of the block that can also make an impact on microclimates (Yin et al., 2019). The formula for calculating shape factor included the area of the block and the perimeter of the block. The grid-level SF was the mean value of each block's shape factor inside the grid. The higher the number, the more elongated or less uniform the block shape is.

Regarding street-related parameters, street height-to-width ratio (H/W) and street orientation are the morphological parameters that most affect microclimates (Ali-Toudert & Mayer, 2006; Chatzidimitriou & Yannas, 2017). Street polygons were converted to centreline. All street polylines were clipped at vertices. To calculate H/W, the height of a street canyon was considered to be the MBH of the closest block, and the width of the street canyon was estimated as twice the distance between the street and the closest building. To calculate street orientation, the

linear directional mean function was used. Every 45 degrees were regarded as one direction. For example, the range between northwest 22.5° and northeast 22.5° was considered as the direction of north. Besides, given the fact that the total length of streets of a neighbourhood, or street density, can also influence connectivity and airflows (Knight & Marshall, 2015), street total length (SL) was also listed as one of the street-related parameters, which was analysed using the total length of streets for each grid.

Regarding vegetation-related parameters, the influential factors include green space and canopy ratio of greenery (Rahman et al., 2019; Rakoto et al., 2021). To reflect these two factors, green space area (AGS) and tree cover ratio (TCR) were adopted in the analysis. AGS was calculated as the total area of green space inside the grid. TCR was a factor measured by the percentage of a grid covered by tree canopy.

It was then necessary to identify the representative combinations of the neighbourhood parameters. As the category that each data should fall into is unknown, unsupervised cluster analysis (James et al., 2013) was used. Cluster analysis is a statistical method used to find similarities between instances in order to group them into classes: the greater the similarity (or homogeneity) within a class and the greater the difference between classes, the better (or more distinct) the clustering solution (Berghauser Pont et al., 2019).
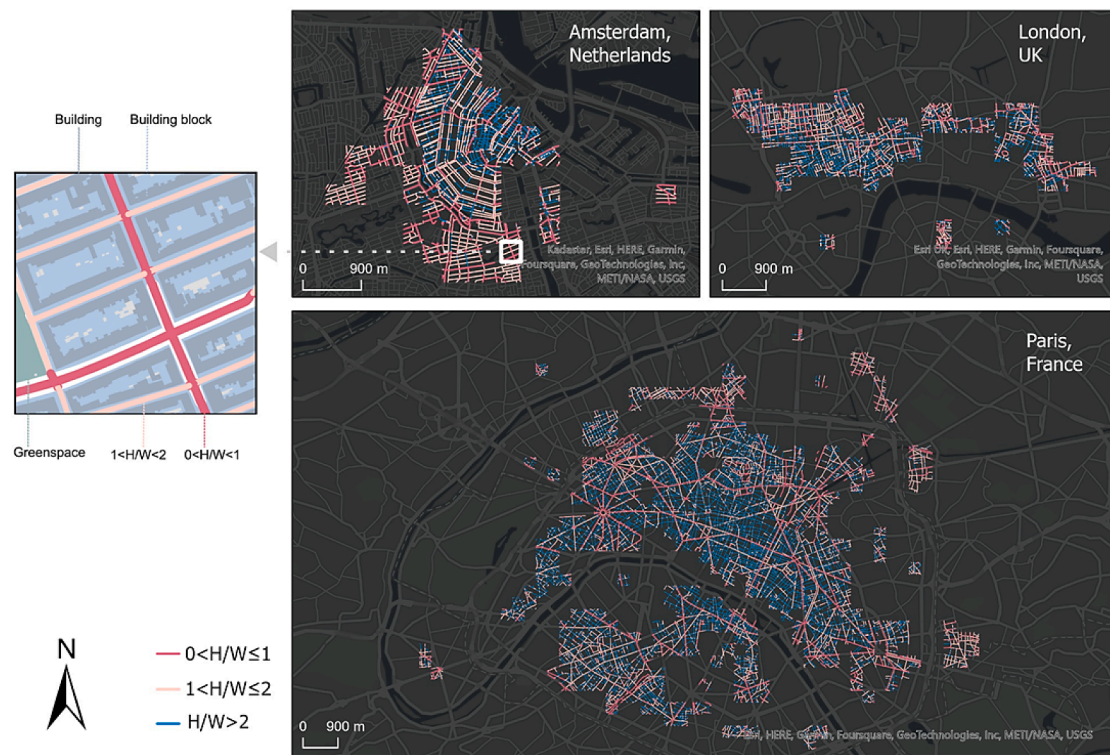
Fig. 4. Height-to-Width ratio distribution in Amsterdam, London, and Paris.

K-means is a cluster analysis algorithm and is the most commonly used approach to produce tighter clusters for large datasets (Kodinariya & Makwana, 2013). In previous studies, Song and Knaap (2007) utilised the K-means cluster analysis to identify distinct neighbourhood types in Portland. Schirmer and Axhausen (2019) utilised the K-means to characterize the 15 attributes concerning building, block, and streets into different urban forms at different scales. Thus, this study adopted K-means for cluster analysis.

The first step of this approach is to transform all the selected parameters into a standardized format (Z-score) for a better outcome (Paul & Sen, 2018). The number of clusters was chosen based on two criteria: the value of Akaike's information criterion (AIC) and Schwarz's Bayesian criterion (BIC) (Kodinariya & Makwana, 2013; Li & Quan, 2020). TwoStep cluster analysis was used to calculate the AIC and BIC. The final clusters were obtained, and the F-value, the distance between each case and the cluster centre was also calculated.

It should be noted that in the cluster analysis, the parameters of CAO and H/W need to be categorised as they have many variations inside one neighbourhood. The orientation was divided into four categories (North-South, East-West, Northwest-Southeast, Northeast-Southwest) with each direction ranging 45 degrees. And according to previous studies, H/W can be divided into three groups that have significant differences in microclimates: 0<H/W≤1, 1<H/W≤2, and H/W>2 (Ali-Toudert & Mayer, 2006). Thus, in the final cluster analysis, we used four variables to describe CAO and three variables to describe H/W.

3. Results and discussion

3.1. Heat-prone local climate zone type

Regarding the LST distribution, it could be found that in general London and Paris have more severe heat problems in the daytime than Amsterdam (Fig. 3, a-c). But the nighttime heat problems in London are less severe as opposed to in Amsterdam and Paris (Fig. 3, e-g). As shown in the LCZ distribution map (Fig. 3, i-k), 11 types of LCZ are found in the

selected three cities. The boxplots of the relationship between LST and LCZ show that LCZ 2 is hottest both in the daytime (Fig. 3, d) and nighttime (Fig. 3, h). By comparing the means of LST using post-hoc Bonferroni test, it shows that LCZ 2 in the nighttime is more prominently problematic than other LCZs (Table A.2), while in the daytime the difference is not significant (Table A.1). According to Bechtel et al. (2019), who analysed 50 cities on the relations between LCZ and LST, it was found that LCZs 2, 3, 8 at daytime and LCZ 1,2 at night time are warmest in general, which is in line with the most heat-prone types identified in this study. LCZ 1-compact high-rise, which usually only consists of small patches in central business districts, is not present in the three cities, so this type is not discussed in this study. LCZ 2-compact mid-rise has the highest mean LST, which can be explained by the high compactness, anthropogenic heat, the lack of greening, and construction materials (Cai et al., 2018; Yang et al., 2021). Benjamin et al. (2021) analysed LCZs in London and also showed that LCZ 2 is the warmest, which is consistent with our results. The reason that LCZ 3 is a lot lower than LCZ 2 in our analysis can be partially explained by the limited presence of LCZ 3 in the three cities (Table B.1). LCZ 5 and LCZ 8 are colder than LCZ 2 considering the lower level of human activity and the increased vegetation coverage. Thus, from this analysis, it can be concluded that LCZ 2-compact mid-rise is the most heat-prone LCZ in the three cities of London, Paris and Amsterdam.

The results of surface albedo (Fig. 3, l-n) show that the LCZ 2, which is regarded as homogeneous areas in LCZ classification, has a rather constant surface albedo value of 0.091-0.125. This analysis provides a more detailed range compared to the LCZ classification, and it proves that the average surface albedo remains constant in LCZ 2. Hence, this parameter will not be included in the next analysis steps but only the seven morphological parameters are to be examined.

3.2. Most frequent combinations of neighbourhood parameters

Regarding the LCZ parameter performance in LCZ 2 (Table C.1), it could be found that in average, the ratio of building plan area to total

Table 3
The descriptive statistics of the neighbourhood morphological variables.

Variable	Minimum	Maximum	Mean	Std. Deviation
SF	1.16	2.19	1.39	0.13
FAR	1.69	8.34	4.53	1.13
SL	489.00	4614.00	2421.05	556.17
P_{N-S}	0.00	0.78	0.23	0.16
P_{E-W}	0.00	0.80	0.24	0.18
P_{NW-SE}	0.00	0.75	0.26	0.17
P_{NE-SW}	0.00	0.80	0.27	0.18
$P_{0<H/W\leq1}$	0.00	0.80	0.17	0.14
$P_{1<H/W\leq2}$	0.02	0.93	0.34	0.15
$P_{H/W>2}$	0.00	0.98	0.49	0.21
TCR	0.00	18.00	5.98	1.96
AGS	0.00	17812.47	2125.31	3666.40

Table 4
Final cluster centres showing the values of each neighbourhood morphological variables.

Variable	Cluster				F-value
	1	2	3	4	
FAR	3.2	4.9	4.9	3.7	115.3***
SF	1.5	1.4	1.4	1.5	35.5***
SL	2310	2414	2573	2146	17.2***
P_{N-S}	36.6%	36.2%	10.4%	14.1%	296.8***
P_{E-W}	48.7%	35.5%	10.5%	18.1%	378.6***
P_{NW-SE}	7.3%	14.8%	39.1%	30.7%	259.2***
P_{NE-SW}	7.4%	13.5%	40.0%	37.1%	311.5***
$P_{0<H/W\leq1}$	27.0%	12.2%	10.4%	38.0%	235.4***
$P_{1<H/W\leq2}$	53.2%	30.8%	30.6%	33.2%	72.0***
$P_{H/W>2}$	19.8%	57.0%	59.0%	28.7%	252.8***
TCR	7.9%	5.4%	5.8%	6.1%	38.7***
AGS	1448	1761	1885	3973	11.3***
Number of cases	80	213	258	105	
	In total 656				

*** The mean difference is significant at the 0.001 level.

plan area is 60.0 %, which is compact and within the range of 40-70 % in the LCZ classification (Stewart & Oke, 2012). The average building height is 22.4 metres, which is mid-rise and within the range of 10-25 metres in the LCZ classification. The AHF is 88.9 Wm^{-2}, which is higher than the range of <75 Wm^{-2} in the classification, indicating that the LCZ 2 in the three cities has a high level of human activities that produce local heating of the atmosphere.

The urban analysis for the morphological parameters that are not included in the LCZ scheme was then carried out within LCZ 2 in the three cities. The street H/W distribution map as an example shows that their combinations are varied in different areas of LCZ 2 (Fig. 4). Other parameters analysed in this study are included in Appendix D (Fig. D.1-D.4). The descriptive statistics present all the parameters used in the cluster analysis (Table 3).

To examine the most frequent combinations of parameters at a neighbourhood level, a K-means cluster analysis for all 12 variables was conducted, including the building block's shape factor and floor area ratio, percentage of four street orientations, percentage of three street H/W categories, street length, area of green space and tree cover ratio.

Using the K-means analysis, the maximum iteration number was set as 30, as our result shows that the change of cluster centre will stop after 22 iterations. Using Akaike's information criterion and Bayesian inference criterion, it was found that the best K number is 4. With the input of K=4 and the 12 variables, the results show that the p-value of all variables is less than 0.001 and case numbers are relatively evenly distributed in each cluster (Table 4).

Final cluster centres (Table 4 and Fig. 5) provide information on each parameter's value for the final typologies. Each cluster represents one typology. In total, there are 656 neighbourhoods analysed in this study, including Cluster 1 (Typology 1) of 80 cases, Cluster 2 (Typology 2) of 213 cases, Cluster 3 (Typology 3) of 258 cases, and Cluster 4 (Typology 4) of 105 cases. In general, Typology 1 has building blocks with lower FAR and more irregular or elongated block shape, mainly consists of N-S and E-W streets, and has more wide street canyons, less green space area but more canopy cover. Typology 2 has building blocks with higher FAR and less irregular or elongated block shape, mainly consists of N-S and E-W streets, and has more narrow street canyons, medium green space area but less canopy cover. Typology 3 has building blocks with higher FAR and less irregular or elongated block shape, mainly consists of NW-SE and NE-SW streets, has more narrow street canyons, longer street total length, less green space area and less canopy cover. Typology 4 has building blocks with lower FAR and more irregular or elongated block shape, streets with all four directions, more wide street canyons, shorter street total length, more green space area and less canopy cover. Regarding the main differences between the four typologies, they are named as Typology 1-Orthogonal 0°-Shallow (mainly wide streets with N-S and E-W orientations), Typology 2-Orthogonal 0°-Deep (mainly narrow streets with N-S and E-W orientations), Typology 3-Orthogonal 45°-Deep (mainly narrow streets with NE-SW and NW-SE orientations), and Typology 4-Cross-Shallow (mainly wide streets with four orientations divided by 45°), separately.

Regarding the difference in the value of each variable, it was found that the F-value of the ANOVA test is different across the clusters (Table 4). Most variations are from the parameters of street orientation and street H/W. Among them, $P_{1<H/W\leq2}$ is less variable across these typologies, indicating that for the four typologies the percentages of street canyons of $1<H/W\leq2$ are comparatively similar to each other, while the percentage of other H/Ws and orientations are more variable. Different percentages of street orientations and H/Ws result in different neighbourhood layouts, and the possible design interventions for the available open space inside these neighbourhoods can thus be different. The rest of the parameters are less effective in explaining the difference across four typologies. Building block's floor area ratio (FAR) is another factor that results in variance between the typologies with comparatively high F-value, followed by tree cover ratio, building block's shape factor, street total length and green space area.

Regarding the spatial and numerical distribution of the typology types, it was found that the three cities have different patterns (Fig. 6, top and bottom left). About half of the neighbourhoods (56%) in Amsterdam are Typology 1, which are distributed in most areas of LCZ 2.
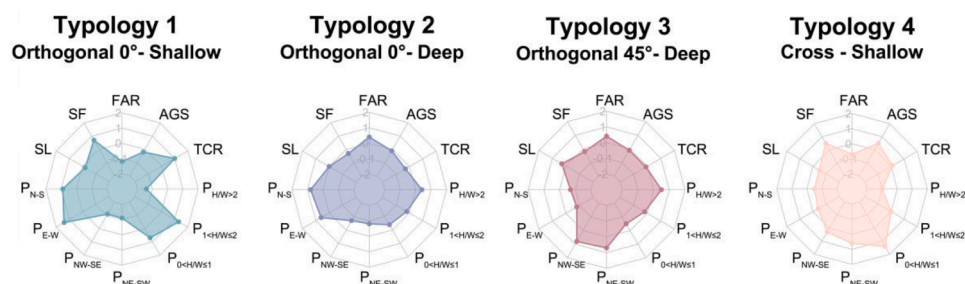

Fig. 5. Radar chart of the values of final cluster centres for the four typologies. Each chart shows the standardised z-score value for all 12 variables.
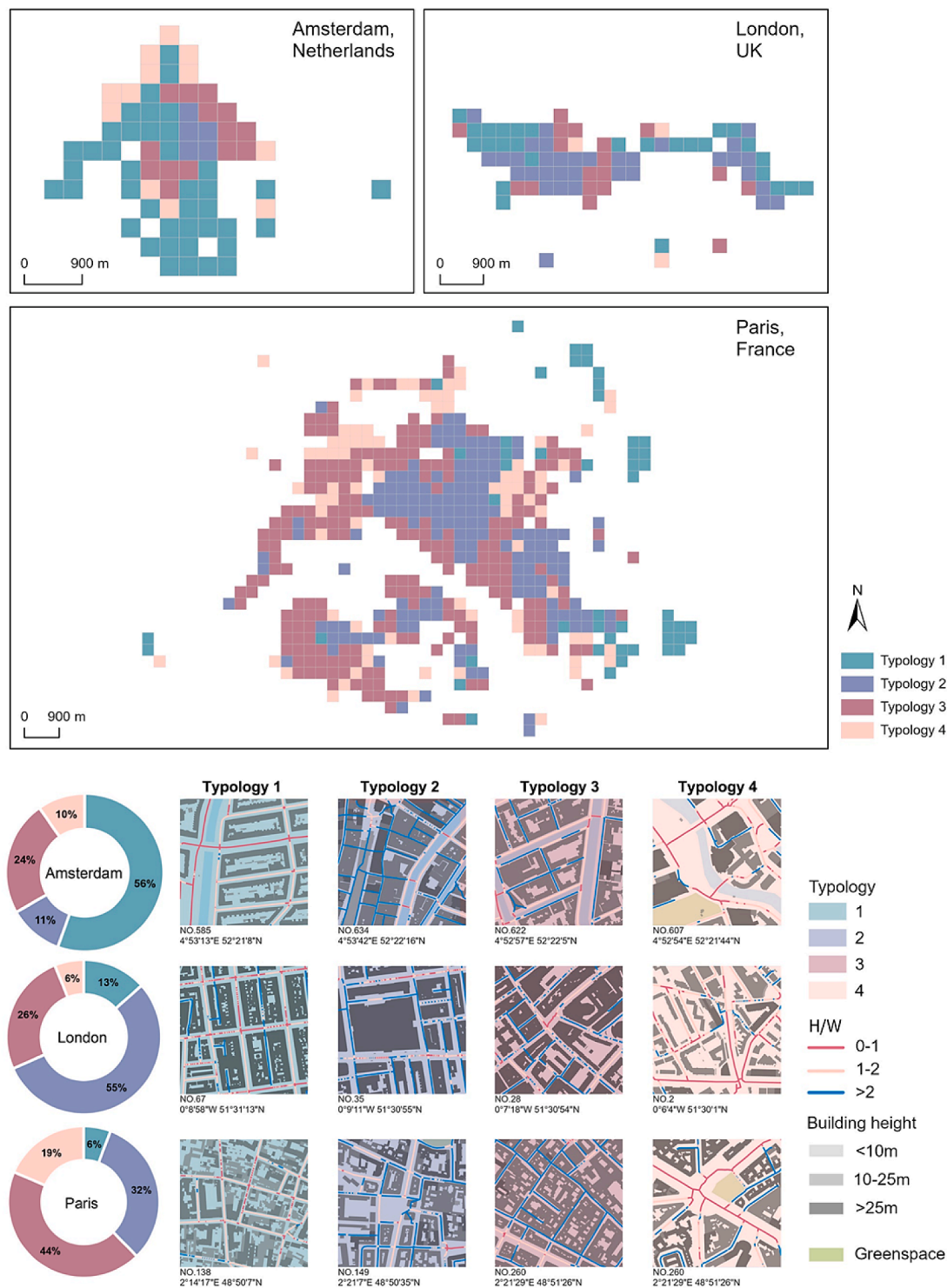
Fig. 6. Typology type distribution map of the three cities (top); Numerical distribution of typology types in the three cities shown in the circle charts (bottom left); Representative real-world examples in the three cities (bottom right).

Typology 3 has the second largest number of typology cases in Amsterdam, followed by Typology 2 and 4. London has half of the neighbourhoods (55%) with Typology 2, followed by Typology 3, 1, and 4. Paris has 44% of Typology 3 and 32% of Typology 2, followed by Typology 4 and Typology 1. The only limited Typology 1 in Paris is located mostly in the periphery of LCZ 2.

More explanations of morphological features of the four typologies can be generated from real-world examples (Fig. 6, bottom right). The FAR in Typology 1 is lower as the building cover ratio (BCR) and mean

building height (MBH) is lower in Amsterdam. The shape factor is higher due to the more elongated perimeter block in Amsterdam. Also, the street tree coverage in Amsterdam is higher than in the other two cities. Typology 2 and 3 mainly consist of narrow street canyons located in the city core of Paris and London. Typology 4 is seen around the roundabouts where main boulevards intersect. The shape factor is also higher due to the existence of irregular courtyards located in Paris, as some of the Haussmann blocks are multi-sided instead of rectangles (Jallon, 2017).
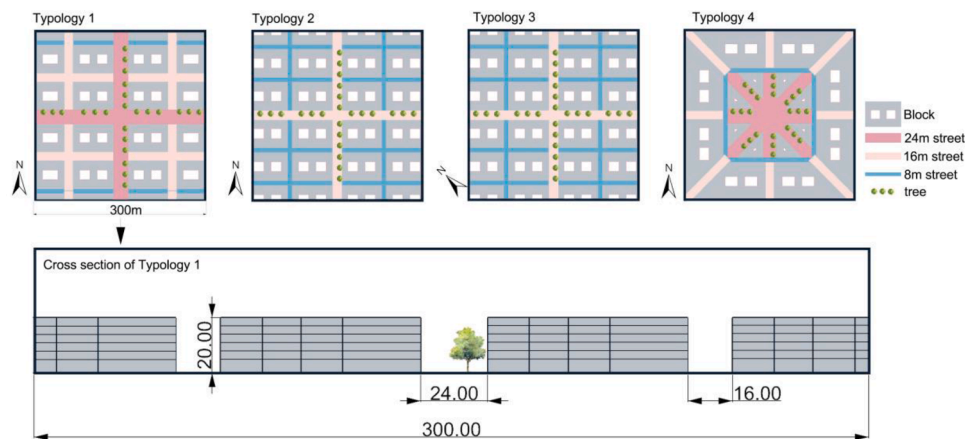
Fig. 7. Generic neighbourhood typologies (top); Cross section of the E-W 24m street in typology 1 (bottom).

Based on the above cluster centres and real-world examples, approximate generic typologies can be proposed (Fig. 7). According to the final cluster centres and the F-values (Table 4), the percentage of street canyon orientation, percentage of street canyon H/W, and vegetation cover are the main parameters to generate neighbourhood typologies. Street canyon width is accordingly set as 24 metres, 16 metres, and 8 metres with regard to the H/W categories of $0<H/W\leq1$, $1<H/W\leq2$, and $H/W>2$. Six-floor buildings are used to represent the 20-metre height. The rectangular building block is 72 metres x 50 metres considering the average street total length, building block size (Fig. C.1) and shape factor.

As shown by the onsite measurements and simulations from previous studies, the different neighbourhood layouts, concerning the combined effects from street orientations of only N-S or both N-S and E-W, the H/Ws ranging from 0.5 to 2, street with or without trees, street total length, and building block's shape in different neighbourhoods, can result in different microclimate variations across neighbourhoods (Yin et al., 2019). Onsite measurements also show that areas with the same street profile but in different neighbourhoods have different thermal sensation performances, if the two neighbourhoods vary in terms of building density, street H/W, street orientation, street trees, and green space (Elbondira et al., 2021). Based on the above facts, it can be concluded that the combined effects of our selected morphological parameters can have an impact on the variations of microclimates across the four neighbourhood typologies.

3.3. Originality of this study

In this study, a novel methodological framework to identify neighbourhood typologies is proposed, starting from the relation of LCZ and LST, down to the neighbourhood-level cluster analysis for parameters that influence microclimates. The generalisation from real-world neighbourhoods to generic typologies bridges the gap between research and practice. Instead of proposing neighbourhood typologies from expert consultation or directly choosing one real neighbourhood, the present study uses a much larger area of three cities (in total 656 neighbourhoods) to generalise the results, making the proposed typologies more applicable in a wider range of future design projects. This provides a common language for future research to analyse thermal sensation at the neighbourhood scale, or to propose cooling and energy-saving design strategies adapted to each typology. This will help

contribute to habitability and sustainability, meeting the sustainable cities and communities development goals (Khosla et al., 2021; Liu et al., 2021). Besides, not only can this methodology be applied in Western Europe, but also in other geographical or climatic contexts. Especially with severe heatwaves occurring across the world more often, these generic heat-prone neighbourhood typologies are in urgent need for different stakeholders to take action.

Additionally, this study adds more detail to the LCZ framework as micro-scale microclimate-related urban design parameters are analysed within a specific LCZ. Synergistic effects among different parameters are complex at the neighbourhood level (Yin et al., 2019). The seven detailed urban design parameters, such as block's FAR, block's shape factor, street orientations, street H/W, street total length, green space area and tree canopy cover included in this study, make the resulting typologies more closely related to real-world neighbourhoods and therefore more useful to inform real-world urban design solutions. With the above taken into account, this study provides new insights to the existing LCZ scheme and acts as a basis for outdoor climate adaptation solutions.

4. Limitations

We acknowledge that there are limitations in this study. Firstly, due to data availability, other European cities with temperate climates were not included in the analysis. The involvement of cities other than Amsterdam, London and Paris in the study could have resulted in differences in the final cluster values and the final typologies. Secondly, to make the typologies more generic, the parameter values adopted are not completely the same as the values of the final cluster centre. For example, when the percentage of $0<H/W\leq1$ is 0.1, which is comparatively negligible compared to $1<H/W\leq2$ and $H/W>2$, it was translated as H/W=0 for simplification, while the real case is more complex than our proposed typologies. Further studies need to find the most typical heat-prone neighbourhood typologies in other geographical or climate contexts so they can be compared, and may use the methodology used in this study. Moreover, statistical analysis between urban heat indicators (LST or thermal comfort indices) and urban design parameters could be further explored. Especially, the comparison of the individual parameters and the typology-based integrated parameters could be interesting for planners in climatic planning.

5. Conclusion

This research is an initial attempt to identify representative neighbourhood typologies that capture the different microclimate-related morphological parameters across a large number of neighbourhoods in different cities. This research specifically raised two questions in the process of developing heat-prone neighbourhood typologies: firstly, what is the most heat-prone Local Climate Zone (LCZ) in European cities with temperate climate? Secondly, what are the most frequent neighbourhood typologies within the identified LCZ based on the characteristics of blocks, streets and vegetation?

With regards to question 1, it has been found that LCZ 2-compact mid-rise areas in the three European cities with temperate climates of London, Paris and Amsterdam are most heat-prone based on the relationship between LCZ and LST. With regards to question 2, four heat-prone neighbourhood typologies were identified based on seven detailed morphological parameters, resulting in different combinations of block's FAR and shape factor, street orientations, street H/W, street total length, green space area and tree canopy cover. In particular, the percentage of street canyons orientations and H/Ws are most variant across the neighbourhood typologies. Given the impact of these factors on urban microclimates, the findings of this study suggest that although areas of each LCZ type share similar morphological properties, one-size-fits-all design solutions cannot be adapted for each LCZ type. Based on these findings, design solutions within the LCZ need to pay particular attention to street canyon orientation and height-to-width ratio, and the four typologies proposed in this study pave the way for the elaboration of different design interventions to that end. Designers working on a specific project can refer to a certain typology and plan their interventions accordingly.

The LCZ framework is a useful tool to represent the heterogeneity of urban thermal environments at a larger scale, and it may be extended with sub-LCZs that consider more detailed morphological characteristics of blocks, streets and vegetation. This research provides a first study for such a finer morphology-based classification method to supplement LCZ. The heat-prone neighbourhood typologies proposed in this study are four sub-LCZs within the LCZ 2- compact mid-rise, being: 1) mainly wide streets with N-S and E-W orientations, 2) mainly narrow streets with N-S and E-W orientations, 3) mainly narrow streets with NE-SW and NW-SE orientations, 4) mainly wide streets with four orientations divided by 45°. The seven detailed parameters in addition to LCZ parameters significantly differentiate the areas with the most heat-prone neighbourhoods in European cities with temperate climates. The method developed in this study can also serve to identify heat-prone neighbourhood typologies in other geographical or climate contexts. The generalised neighbourhood typologies can act as the basis for designing future strategies to generate thermally comfortable outdoor space, contributing to a more climate-resilient city under the threat of urban heat stress.

CRediT authorship contribution statement

Yehan Wu: Conceptualization, Data curation, Formal analysis, Methodology, Software, Visualization, Writing – original draft. **Bardia Mashhoodi:** Data curation, Methodology, Software, Supervision, Writing – review & editing. **Agnès Patuano:** Methodology, Supervision, Writing – review & editing. **Sanda Lenzholzer:** Funding acquisition, Project administration, Supervision, Writing – review & editing. **Laura Narvaez Zertuche:** Project administration, Supervision, Writing – review & editing. **Andy Acred:** Project administration, Supervision, Writing – review & editing.

Declaration of Competing Interest

The authors declare that they have no known competing financial interests or personal relationships that could have appeared to influence the work reported in this paper.

Data Availability

Data will be made available on request.

Acknowledgements

Appendix A. Bonferroni test

Table A1, Table A2

Table A1
Post-hoc Bonferroni test comparing the means of daytime LST.

	LCZ 3	LCZ 5	LCZ 6	LCZ 8	LCZ A	LCZ B	LCZ D	LCZ E	LCZ F
LCZ 2	1.000	1.000	***	*	***	***	***	1.000	***
LCZ 3		1.000	1.000	1.000	***	**	***	1.000	***
LCZ 5			***	*	***	***	***	1.000	***
LCZ 6				1.000	***	***	***	1.000	***
LCZ 8					***	***	***	1.000	***
LCZ A						**	*	0.755	1.000
LCZ B							***	1.000	*
LCZ D								0.056	1.000
LCZ E									0.225

* The mean difference is significant at the 0.05 level.
** The mean difference is significant at the 0.01 level.
*** The mean difference is significant at the 0.001 level.

Table A2
Post-hoc Bonferroni test comparing the means of nighttime LST.

	LCZ 3	LCZ 5	LCZ 6	LCZ 8	LCZ A	LCZ B	LCZ D	LCZ E	LCZ F
LCZ 2	***	***	***	***	***	***	***	**	***
LCZ 3		***	1.000	**	1.000	1.000	0.696	1.000	1.000
LCZ 5			***	1.000	***	***	***	1.000	1.000
LCZ 6				***	0.308	***	***	1.000	1.000
LCZ 8					***	***	***	1.000	1.000
LCZ A						***	***	1.000	0.062
LCZ B							1.000	1.000	***
LCZ D								1.000	***
LCZ E									1.000

* The mean difference is significant at the 0.05 level.
** The mean difference is significant at the 0.01 level.
*** The mean difference is significant at the 0.001 level.

Appendix B. LCZ frequency

Table B1

Table B1
The frequency of LCZ types of the three cities.

LCZ type	Frequency	Percent	Valid Percent	Cumulative Percent
2	149	4.4	4.4	4.4
3	20	0.6	0.6	5
5	320	9.6	9.6	14.6
6	1767	52.7	52.7	67.3
8	247	7.4	7.4	74.7
9	1	0	0	74.7
11	179	5.3	5.3	80.1
12	404	12.1	12.1	92.1
14	223	6.7	6.7	98.8
15	6	0.2	0.2	99
17	34	1	1	100
Total	3350	100	100	

Appendix C. Values of LCZ parameters

Table C1, Fig. C1

Table C1
Descriptive analysis of LCZ parameters.

LCZ parameters	Minimum	Maximum	Mean	Std. Deviation
Ratio of building plan area to total plan area (%)	0	100.0	60.0	13.0
Building height (m)	0	113.5	22.4	6.9
Anthropogenic heat flux (Wm^{-2})	1.5	227.8	88.9	53.8
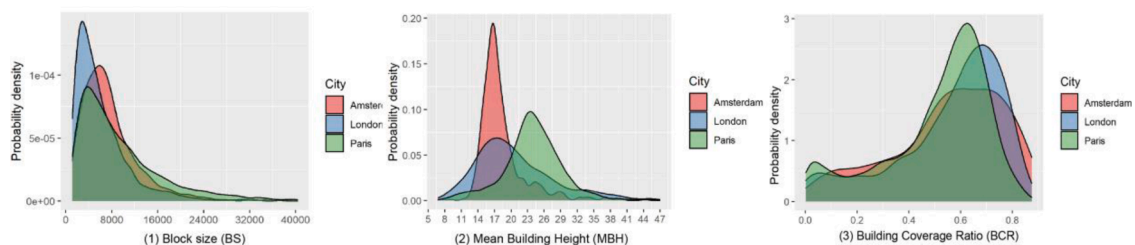
Fig. C1. Probability density figures of block size, mean building height, and building coverage ratio of the building blocks in the LCZ 2 of the three cities.

Appendix D. Maps of different parameters analysed in this study

Fig. D1. Building coverage ratio (BCR) and building height in Amsterdam, London, and Paris.
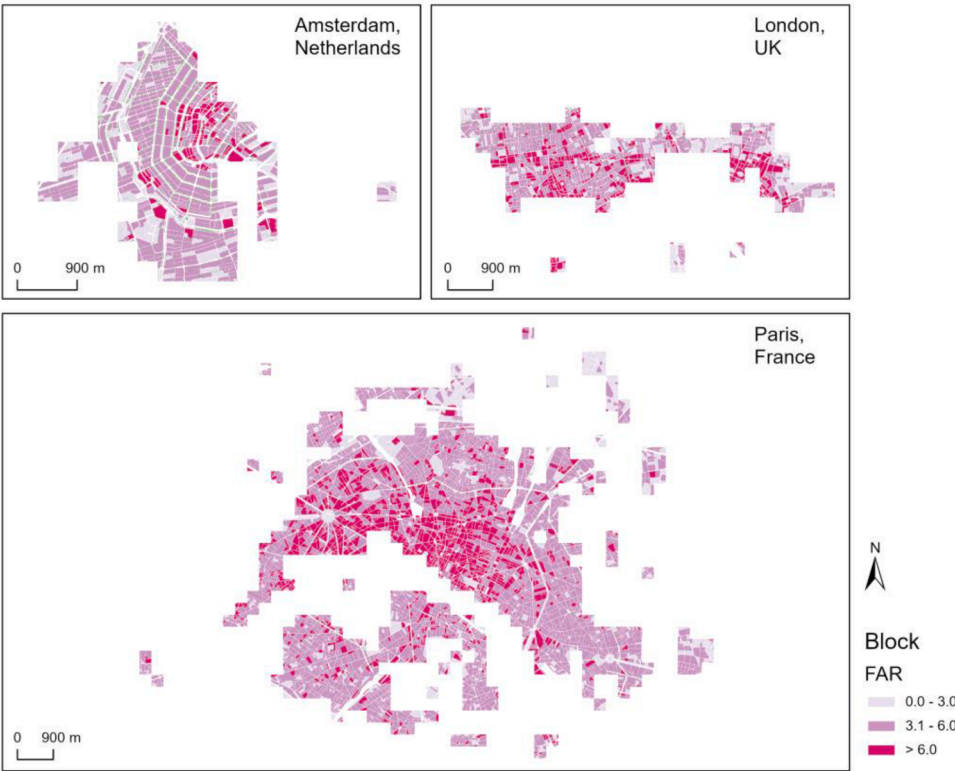

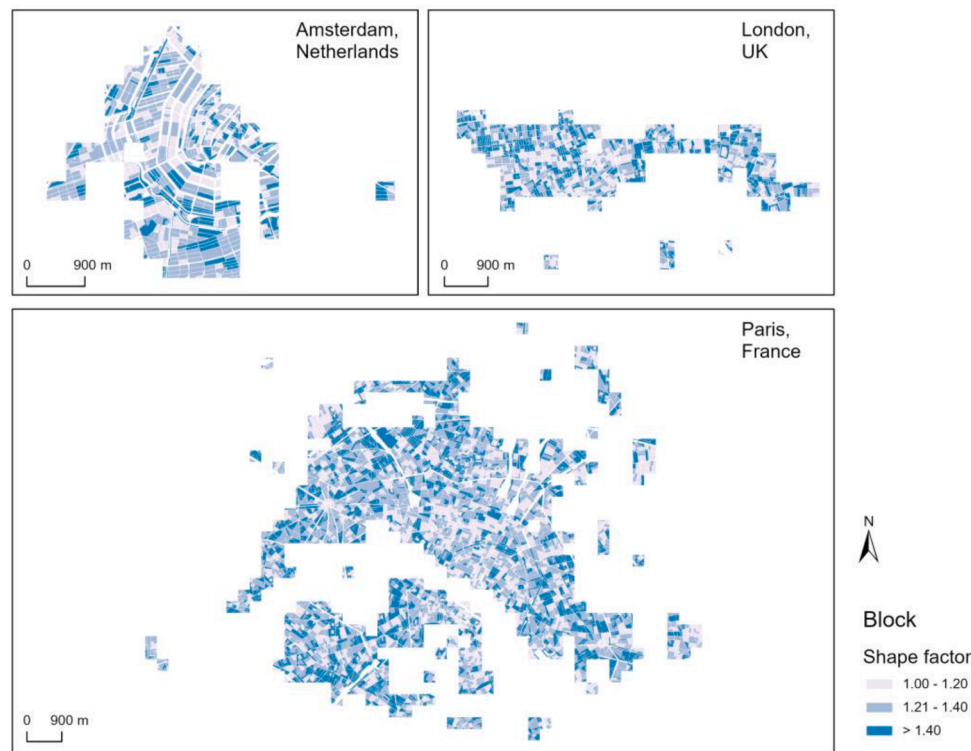**Fig. D2.** Building block's floor area ratio (FAR) in Amsterdam, London, and Paris.

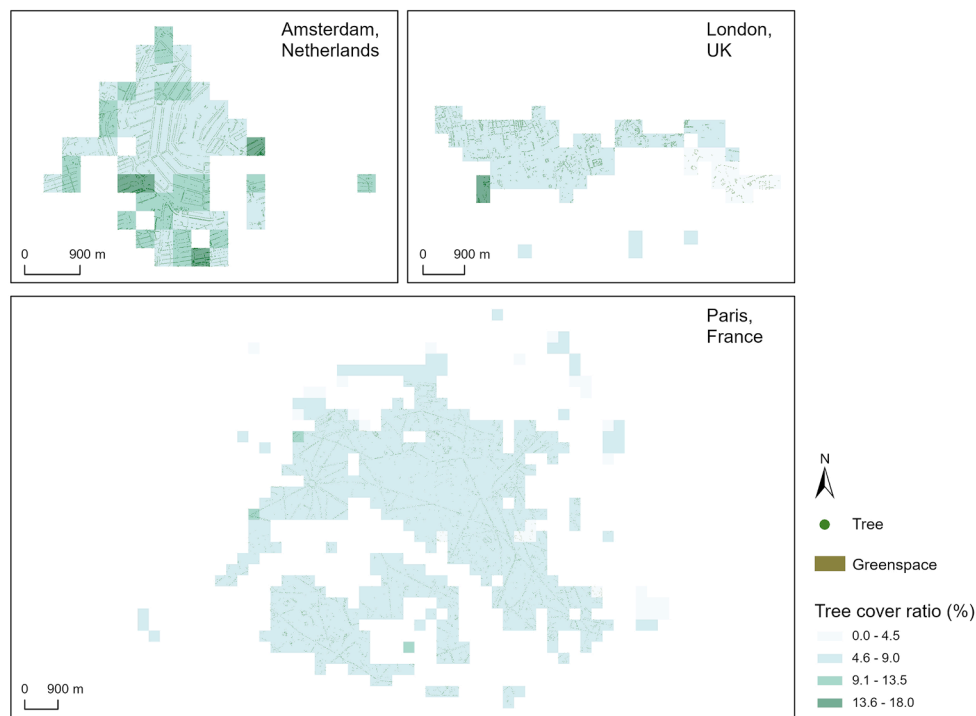**Fig. D3.** Building block's shape factor in Amsterdam, London, and Paris.

Fig. D4. Tree, greenspace and tree cover ratio in Amsterdam, London, and Paris.

References

Aboelata, A. (2020). Vegetation in different street orientations of aspect ratio (H/W 1:1) to mitigate UHI and reduce buildings' energy in arid climate. *Building and Environment, 172*, Article 106712. https://doi.org/10.1016/j.buildenv.2020.106712

Aghamolaei, R., Azizi, M. M., Aminzadeh, B., & Mirzaei, P. A. (2020). A tempo-spatial modelling framework to assess outdoor thermal comfort of complex urban neighbourhoods. *Urban Climate, 33*, Article 100665. https://doi.org/10.1016/j.uclim.2020.100665

Aleksandrowicz, O., Vuckovic, M., Kiesel, K., & Mahdavi, A. (2017). Current trends in urban heat island mitigation research: Observations based on a comprehensive research repository. *Urban Climate, 21*, 1–26. https://doi.org/10.1016/j.uclim.2017.04.002

Ali-Toudert, F., & Mayer, H. (2006). Numerical study on the effects of aspect ratio and orientation of an urban street canyon on outdoor thermal comfort in hot and dry

climate. *Building and Environment, 41*(2), 94–108. https://doi.org/10.1016/j. buildenv.2005.01.013

Amani-Beni, M., Zhang, B., Xie, G., & Xu, J. (2018). Impact of urban park's tree, grass and waterbody on microclimate in hot summer days: A case study of Olympic Park in Beijing, China. *Urban Forestry & Urban Greening, 32*, 1–6. https://doi.org/10.1016/j. ufug.2018.03.016

Aminipouri, M., Knudby, A. J., Krayenhoff, E. S., Zickfeld, K., & Middel, A. (2019). Modelling the impact of increased street tree cover on mean radiant temperature across Vancouver's local climate zones. *Urban Forestry & Urban Greening, 39*, 9–17. https://doi.org/10.1016/j.ufug.2019.01.016

Atelier Parisien d'Urbanisme. (2020). PLU HAUTEUR. https://opendata.apur.org/dat asets/-Apur::plu-hauteur/explore.

Bartesaghi-Koc, C., Osmond, P., Peters, A., & Irger, M. (2018). Understanding land surface temperature differences of local climate zones based on airborne remote sensing data. *IEEE Journal of Selected Topics in Applied Earth Observations and Remote Sensing, 11*(8), 2724–2730. https://doi.org/10.1109/jstars.2018.2815004

Bechtel, B., & Daneke, C. (2012). Classification of local climate zones based on multiple earth observation data. *IEEE Journal of Selected Topics in Applied Earth Observations and Remote Sensing, 5*(4), 1191–1202.

Bechtel, B., Demuzere, M., Mills, G., Zhan, W., Sismanidis, P., Small, C., & Voogt, J. (2019). SUHI analysis using local climate zones—A comparison of 50 cities. *Urban Climate, 28*, Article 100451. https://doi.org/10.1016/j.uclim.2019.01.005

Beck, H. E., Zimmermann, N. E., McVicar, T. R., Vergopolan, N., Berg, A., & Wood, E. F. (2018). Present and future Köppen-Geiger climate classification maps at 1-km resolution. *Scientific Data, 5*(1), Article 180214. https://doi.org/10.1038/sdata.2018.214

Benjamin, K., Luo, Z., & Wang, X. (2021). Crowdsourcing urban air temperature data for estimating urban heat island and building heating/cooling load in London. *Energies, 14*(16), 5208. https://doi.org/10.3390/en14165208

Berghauser Pont, M., Stavroulaki, G., Bobkova, E., Gil, J., Marcus, L., Olsson, J., Sun, K., Serra, M., Hausleitner, B., Dhanani, A., & Legeby, A. (2019). The spatial distribution and frequency of street, plot and building types across five European cities. *Environment and Planning B: Urban Analytics and City Science, 46*(7), 1226–1242. https://doi.org/10.1177/2399808319857450

Brown, R. D. (2010). *Design with microclimate: The secret to comfortable outdoor space.* Island Press.

Cai, M., Ren, C., Xu, Y., Lau, K. K. L., & Wang, R (2018). Investigating the relationship between local climate zone and land surface temperature using an improved WUDAPT methodology – A case study of Yangtze River Delta, China. *Urban Climate, 24*, 485–502. https://doi.org/10.1016/j.uclim.2017.05.010

Chatzidimitriou, A., & Yannas, S. (2017). Street canyon design and improvement potential for urban open spaces; the influence of canyon aspect ratio and orientation on microclimate and outdoor comfort. *Sustainable Cities and Society, 33*, 85–101. https://doi.org/10.1016/j.scs.2017.05.019

Chen, Y., Zheng, B., & Hu, Y. (2020). Numerical simulation of local climate zone cooling achieved through modification of trees, albedo and green roofs—a case study of Changsha. *China. Sustainability, 12*(7), 2752.

Climate.onebuilding.org. Retrieved 1 June 2021, from https://climate.onebuilding.org/.

Cohen, P., Potchter, O., & Matzarakis, A. (2012). Daily and seasonal climatic conditions of green urban open spaces in the Mediterranean climate and their impact on human comfort. *Building and Environment, 51*, 285–295. https://doi.org/10.1016/j. buildenv.2011.11.020

Demuzere, M., Bechtel, B., Middel, A., & Mills, G. (2019). Mapping Europe into local climate zones. *PLOS ONE, 14*(4), Article e0214474. https://doi.org/10.1371/journal.pone.0214474

Demuzere, M., Kittner, J., Martilli, A., Mills, G., Moede, C., Stewart, I. D., van Vliet, J., & Bechtel, B. (2022). A global map of Local Climate Zones to support earth system modelling and urban scale environmental science. *Earth System Science Data Discussions*, 1–57. https://doi.org/10.5194/essd-2022-92

Deilami, K., Kamruzzaman, M., & Liu, Y. (2018). Urban heat island effect: A systematic review of spatio-temporal factors, data, methods, and mitigation measures. *International Journal of Applied Earth Observation and Geoinformation, 67*, 30–42.

DiMiceli, Charlene, Carroll, Mark, Sohlberg, Robert, Kim, Do-Hyung, Kelly, Maggi, & Townshend, John (2015). *MOD44B MODIS/terra vegetation continuous fields yearly L3 global 250m SIN Grid V006 [Data set]*. NASA EOSDIS Land Processes DAAC. https://doi.org/10.5067/MODIS/MOD44B.006

Elbondira, T. A., Tokimatsu, K., Asawa, T., & Ibrahim, M. G. (2021). Impact of neighborhood spatial characteristics on the microclimate in a hot arid climate – A field based study. *Sustainable Cities and Society, 75*, Article 103273. https://doi.org/10.1016/j.scs.2021.103273

Eldesoky, A. H., Gil, J., & Pont, M. B. (2022). Combining Environmental and Social Dimensions in the Typomorphological Study of Urban Resilience to Heat Stress. Sustainable Cities and Society, 103971. https://doi.org/10.1016/j.scs.2022.103971.

Erell, E. (2008). The application of urban climate research in the design of cities. *Advances in Building Energy Research, 2*(1), 95–121.

Froment H, Below R (2020) CRED crunch 58 - disaster year in review 2019. 58.

Hidalgo, J., Lemonsu, A., & Masson, V. (2018). Between progress and obstacles in urban climate interdisciplinary studies and knowledge transfer to society. *Annals of the New York Academy of Sciences, 1436*(1), 5–18. https://doi.org/10.1111/nyas.13986

Jallon, B. (2017). *Paris Haussmann. A model's relevance.* Park Books.

James, G., Witten, D., Hastie, T., & Tibshirani, R. (2013). *An introduction to statistical learning* (Vol. 112). Springer.

Khosla, R., Miranda, N. D., Trotter, P. A., Mazzone, A., Renaldi, R., McElroy, C., Cohen, F., Jani, A., Perera-Salazar, R., & McCulloch, M. (2021). Cooling for sustainable development. *Nature Sustainability, 4*(3), 201–208.

Kim, S. W., & Brown, R. D. (2022). Pedestrians' behavior based on outdoor thermal comfort and micro-scale thermal environments, Austin, TX. *Science of The Total Environment, 808*, Article 152143. https://doi.org/10.1016/j.scitotenv.2021.152143

Klemm, W., Heusinkveld, B. G., Lenzholzer, S., & van Hove, B. (2015). Street greenery and its physical and psychological impact on thermal comfort. *Landscape and Urban Planning, 138*, 87–98. https://doi.org/10.1016/j.landurbplan.2015.02.009

Knight, P. L., & Marshall, W. E. (2015). The metrics of street network connectivity: Their inconsistencies. *Journal of Urbanism: International Research on Placemaking and Urban Sustainability, 8*(3), 241–259.

Kodinariya, T. M., & Makwana, P. R. (2013). Review on determining number of Cluster in K-Means Clustering. *International Journal, 1*(6), 90–95.

Lenzholzer, S. (2015). *Weather in the City-how design shapes the urban climate.* Nai 010 Uitgevers/Publishers.

Lenzholzer, S., & Brown, R. D. (2016). Post-positivist microclimatic urban design research: A review. *Landscape and Urban Planning, 153*, 111–121.

Li, N., & Quan, S. J. (2020). Identifying urban form typologies in seoul with mixture model based clustering. https://doi.org/10.13140/RG.2.2.20864.46088.

Liang, S. (2001). Narrowband to broadband conversions of land surface albedo I: Algorithms. *Remote Sensing of Environment, 76*(2), 213–238. https://doi.org/10.1016/S0034-4257(00)00205-4

Liu, H., Huang, B., Zhan, Q., Gao, S., Li, R., & Fan, Z. (2021). The influence of urban form on surface urban heat island and its planning implications: Evidence from 1288 urban clusters in China. *Sustainable Cities and Society, 71*, Article 102987. https://doi.org/10.1016/j.scs.2021.102987

Liu, Y., Lin, W., Guo, J., Wei, Q., & Shamseldin, A. Y. (2019). The influence of morphological characteristics of green patch on its surrounding thermal environment. *Ecological Enginnering, 140*. https://doi.org/10.1016/j.ecoleng.2019.105594

Louf, R., & Barthelemy, M. (2014). A typology of street patterns. *Journal of The Royal Society Interface, 11*(101), Article 20140924.

Maiullari, D., Esch, M. P., & Timmeren, A.van. (2021). A quantitative morphological method for mapping local climate types. *Urban Planning, 6*(3), 240–257. https://doi.org/10.17645/up.v6i3.4223

Martins, T. A., de, L., Faraut, S., & Adolphe, L. (2019). Influence of context-sensitive urban and architectural design factors on the energy demand of buildings in Toulouse. *France. Energy and Buildings, 190*, 262–278. https://doi.org/10.1016/j.enbuild.2019.02.019

Middel, A., Häb, K., Brazel, A. J., Martin, C. A., & Guhathakurta, S. (2014). Impact of urban form and design on mid-afternoon microclimate in Phoenix Local Climate Zones. *Landscape and Urban Planning, 122*, 16–28. https://doi.org/10.1016/j.landurbplan.2013.11.004

Mitraka, Z., Del Frate, F., Chrysoulakis, N., & Gastellu-Etchegorry, J.-P. (2015). Exploiting earth observation data products for mapping local climate zones. *2015 Joint Urban Remote Sensing Event (JURSE)*, 1–4.

Norton, B. A., Coutts, A. M., Livesley, S. J., Harris, R. J., Hunter, A. M., & Williams, N. S. G. (2015). Planning for cooler cities: A framework to prioritise green infrastructure to mitigate high temperatures in urban landscapes. *Landscape and Urban Planning, 134*, 127–138. https://doi.org/10.1016/j.landurbplan.2014.10.018

Oke, T. R., Mills, G., Christen, A., & Voogt, J. A. (2017). *Urban climates.* Cambridge University Press.

OS MasterMap Building Height Attribute [FileGeoDatabase geospatial data], Scale 1: 2500, Updated: 30 August 2019, Ordnance Survey (GB), Using: EDINA Digimap Ordnance Survey Service, <https://digimap.edina.ac.uk>, Downloaded: 2021-01-29 16:14:46.348.

Pan, W. (2019). *Diverse environmental performances of urban villages and insights for enhancing quality of urban renewal in Shenzhen.* HKU Theses Online (HKUTO).

Pan, W., & Du, J. (2021). Impacts of urban morphological characteristics on nocturnal outdoor lighting environment in cities: An empirical investigation in Shenzhen. *Building and Environment, 192*, Article 107587. https://doi.org/10.1016/j.buildenv.2021.107587

Paul, A., & Sen, J. (2018). Livability assessment within a metropolis based on the impact of integrated urban geographic factors (IUGFs) on clustering urban centers of Kolkata. *Cities, 74*, 142–150. https://doi.org/10.1016/j.cities.2017.11.015

Perini, K., & Magliocco, A. (2014). Effects of vegetation, urban density, building height, and atmospheric conditions on local temperatures and thermal comfort. *Urban Forestry & Urban Greening, 13*(3), 495–506. https://doi.org/10.1016/j.ufug.2014.03.003

Peters, R., Dukai, B., Vitalis, S., van Liempt, J., & Stoter, J. (2021). *ArXiv Preprint.*

Prominski, M. (2016). Design guidelines. *Research in landscape architecture* (pp. 194–208). Routledge.

Rahman, M. A., Moser, A., Rötzer, T., & Pauleit, S. (2019). Comparing the transpirational and shading effects of two contrasting urban tree species. *Urban Ecosystems, 22*(4), 683–697. https://doi.org/10.1007/s11252-019-00853-x

Rakoto, P. Y., Deilami, K., Hurley, J., Amati, M., & Sun, Q. (2021). Revisiting the cooling effects of urban greening: Planning implications of vegetation types and spatial configuration. *Urban Forestry & Urban Greening, 64*, Article 127266. https://doi.org/10.1016/j.ufug.2021.127266

Ramyar, R., Zarghami, E., & Bryant, M. (2019). Spatio-temporal planning of urban neighborhoods in the context of global climate change: Lessons for urban form design in Tehran, Iran. *Sustainable Cities and Society.* Elsevier. https://doi.org/10.1016/j.scs.2019.101554. Vol. 51.

Ratti, C., Raydan, D., & Steemers, K. (2003). Building form and environmental performance: Archetypes, analysis and an arid climate. *Energy and Buildings, 35*(1), 49–59. https://doi.org/10.1016/S0378-7788(02)00079-8

Raymond, C. M., Breil, M., Nita, M. R., Kabisch, N., de Bel, M., Enzi, V., Frantzeskaki, N., Geneletti, G., Lovinger, L., & Cardinaletti, M. (2017). An impact evaluation

framework to support planning and evaluation of nature-based solutions projects. *Report prepared by the EKLIPSE Expert Working Group on Nature-Based Solutions to Promote Climate Resilience in Urban Areas*. Centre for Ecology and Hydrology.

Robine, J.-M., Cheung, S. L. K., Le Roy, S., Van Oyen, H., Griffiths, C., Michel, J.-P., & Herrmann, F. R. (2008). Death toll exceeded 70,000 in Europe during the summer of 2003. *Comptes Rendus Biologies, 331*(2), 171–178. https://doi.org/10.1016/j.crvi.2007.12.001

Rode, P., Keim, C., Robazza, G., Viejo, P., & Schofield, J. (2014). Cities and energy: Urban morphology and residential heat-energy demand. *Environment and Planning B: Planning and Design, 41*(1), 138–162. https://doi.org/10.1068/b39065

Roe, J., & McCay, L. (2021). *Restorative Cities: Urban design for mental health and wellbeing*. Bloomsbury Publishing.

Rousi, E., Kornhuber, K., Beobide-Arsuaga, G., Luo, F., & Coumou, D. (2022). Accelerated western European heatwave trends linked to more-persistent double jets over Eurasia. *Nature Communications, 13*(1), 1–11.

Sangiorgio, V., Fiorito, F., & Santamouris, M. (2020). Development of a holistic urban heat island evaluation methodology. *Scientific Reports, 10*(1), 17913. https://doi.org/10.1038/s41598-020-75018-4

Schaaf, C., & Wang, Z. (2015). *MCD43A3 MODIS/Terra+Aqua BRDF/Albedo Daily L3 Global - 500m V006 [Data set]*. NASA EOSDIS Land Processes DAAC. https://doi.org/10.5067/MODIS/MCD43A3.006 Accessed 2022-08-08 from.

Schirmer, P. M., & Axhausen, K. W. (2019). A multiscale clustering of the urban morphology for use in quantitative models. In L. D'Acci (Ed.), *The Mathematics of Urban Morphology* (pp. 355–382). Springer International Publishing. https://doi.org/10.1007/978-3-030-12381-9_16.

Schwaab, J., Meier, R., Mussetti, G., Seneviratne, S., Bürgi, C., & Davin, E. L. (2021). The role of urban trees in reducing land surface temperatures in European cities. *Nature Communications, 12*(1), 6763. https://doi.org/10.1038/s41467-021-26768-w

Song, Y., & Knaap, G.-J. (2007). Quantitative classification of neighbourhoods: The neighbourhoods of new single-family homes in the portland metropolitan area. *Journal of Urban Design, 12*(1), 1–24. https://doi.org/10.1080/13574800601072640

Srivanit, M., & Jareemit, D. (2020). Modeling the influences of layouts of residential townhouses and tree-planting patterns on outdoor thermal comfort in Bangkok suburb. *Journal of Building Engineering, 30*, Article 101262.

Stewart, I. D., & Oke, T. R. (2012). Local climate zones for urban temperature studies. *Bulletin of the American Meteorological Society, 93*(12), 1879–1900. https://doi.org/10.1175/BAMS-D-11-00019.1

Taleghani, M., Kleerekoper, L., Tenpierik, M., & van den Dobbelsteen, A. (2015). Outdoor thermal comfort within five different urban forms in the Netherlands. *Building and Environment, 83*, 65–78. https://doi.org/10.1016/j.buildenv.2014.03.014

Urban Atlas 2018, Copernicus land monitoring service. [Land item]. (2020). Retrieved 16 December 2021, from https://land.copernicus.eu/local/urban-atlas/urban-atlas-2018

Wan, Z., Hook, S., & Hulley, G. (2015). *MOD11A2 MODIS/Terra land surface temperature/emissivity 8-day L3 global 1km SIN grid V006* (p. 10). NASA EOSDIS Land Processes DAAC.

Witze, A. (2022). Extreme heatwaves: Surprising lessons from the record warmth. *Nature*.

Xu, Y., Ren, C., Ma, P., Ho, J., Wang, W., Lau, K. K. L., Lin, H., & Ng, E. (2017). Urban morphology detection and computation for urban climate research. *Landscape and Urban Planning, 167*, 212–224. https://doi.org/10.1016/j.landurbplan.2017.06.018

Yang, J., Ren, J., Sun, D., Xiao, X., Xia, J, (Cecilia), Jin, C., & Li, X (2021). Understanding land surface temperature impact factors based on local climate zones. *Sustainable Cities and Society, 69*, Article 102818. https://doi.org/10.1016/j.scs.2021.102818

Yao, L., Li, T., Xu, M., & Xu, Y. (2020). How the landscape features of urban green space impact seasonal land surface temperatures at a city-block-scale: An urban heat island study in Beijing, China. *Urban Forestry & Urban Greening, 52*, Article 126704. https://doi.org/10.1016/j.ufug.2020.126704

Yin, S., Lang, W., & Xiao, Y. (2019). The synergistic effect of street canyons and neighbourhood layout design on pedestrian-level thermal comfort in hot-humid area of China. *Sustainable Cities and Society, 49*, Article 101571. https://doi.org/10.1016/j.scs.2019.101571

Yuan, J., Emura, K., & Farnham, C. (2017). Is urban albedo or urban green covering more effective for urban microclimate improvement?: A simulation for Osaka. *Sustainable Cities and Society, 32*, 78–86. https://doi.org/10.1016/j.scs.2017.03.021

Zhang, Y., Murray, A. T., & Turner Ii, B. L. (2017). Optimizing green space locations to reduce daytime and nighttime urban heat island effects in Phoenix. *Arizona. Landscape and Urban Planning, 165*, 162–171.

Zheng, Y., Ren, C., Xu, Y., Wang, R., Ho, J., Lau, K., & Ng, E. (2018). GIS-based mapping of local climate zone in the high-density city of Hong Kong. *Urban Climate, 24*, 419–448. https://doi.org/10.1016/j.uclim.2017.05.008

Ziter, C. D., Pedersen, E. J., Kucharik, C. J., & Turner, M. G. (2019). Scale-dependent interactions between tree canopy cover and impervious surfaces reduce daytime urban heat during summer. In *, 116. Proceedings of the National Academy of Sciences* (pp. 7575–7580).